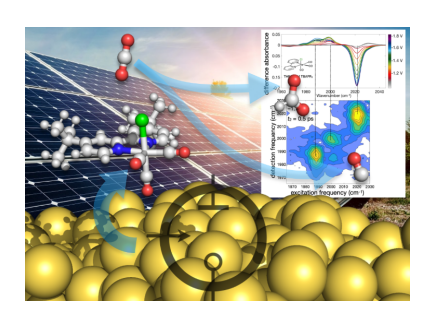
Transmission Mode 2D-IR Spectroelectrochemistry of *In Situ* Electrocatalytic Intermediates

Laura M. Kiefer, Lindsay B. Michocki and Kevin J. Kubarych

Department of Chemistry, University of Michigan, 930 N. University Ave., Ann Arbor, MI 48109, USA

Abstract:

Unraveling electrocatalytic mechanisms, as well as fundamental structural dynamics of intermediates, requires spectroscopy with high time and frequency resolution that can account for non-equilibrium *in situ* concentration changes inherent to electrochemistry. Two-dimensional infrared (2D-IR) spectroscopy is an ideal candidate, but several technical challenges have hindered development of this powerful tool for spectroelectrochemistry (SEC). We demonstrate a transmission-mode, optically transparent thin-layer electrochemical (OTTLE) cell adapted to 2D-IR-SEC to monitor the important Re(bpy)(CO)₃CI CO₂-reduction electrocatalyst. 2D-IR-SEC reveals pronounced differences in both spectral diffusion time scales and spectral inhomogeneity in the singly reduced catalyst, [Re(bpy)(CO)₃CI]⁶⁻, relative to the starting Re(bpy)(CO)₃CI. Crosspeaks between well-resolved symmetric vibrations and congested low-frequency bands enable direct assignment of all distinct species during the electrochemical reaction. With this information, 2D-IR-SEC provides new mechanistic insights regarding unproductive, catalyst degrading dimerization. 2D-IR-SEC opens a new experimental windows into the electrocatalysis foundation of future energy conversion and greenhouse gas reduction.



Spectroelectrochemistry (SEC) combines electrochemical methods with spectroscopic techniques, allowing *in situ* access to electrochemical processes. Electrochemistry is experiencing a major renaissance due to its central role in converting greenhouse gases to useful starting materials and fuel. There are many aspects of traditional and emerging electrochemistry that have yet to be examined with modern tools of physical chemistry, such as ultrafast, multidimensional optical spectroscopy. Spectroelectrochemistry is widely used, incorporating a variety of modalities such as NMR, Raman, UV-vis, and infrared, allowing these electrochemical systems to be viewed from multiple perspectives.[1-5] Only very recently have we seen the introduction of ultrafast spectroscopy to SEC, reporting dynamics of species during

electrochemical reactions, leading to a more complete characterization of multiple redox states.[6] Ultrafast techniques provide access to equilibrium and nonequilibrium solvation, interand intramolecular energy transfer, and possibly chemical exchange.

Two-dimensional infrared spectroscopy (2D-IR) gives valuable insight into ultrafast vibrational dynamics of both the system and its solvent or immediate surroundings, and is a powerful tool for observing phenomena such as preferential solvation, structural dynamics, vibrational energy transfer and relaxation.[7-10] For example, using a dynamical signature of solvent shell exchange, we found that the Re(bpy)(CO)₃Cl CO₂ reduction photocatalyst is most preferentially solvated by the amine electron donor at the optimal conditions for CO₂ reduction to CO.[9] Given the large changes in charge distribution induced by changing the redox state of the molecule, the solvent molecules surrounding the redox system interact differently with different oxidation states, resulting in possible changes to vibrational lifetimes or spectral diffusion timescales that can be revealed using 2D-IR.[11]

Pioneering work by Hamm *et al.*[12-13] and by Bredenbeck *et al.*[6, 14] combining 2D-IR and electrochemistry has employed reflectance geometries, where an electrode serves as both a reflecting or absorption enhancing surface and the working electrode.[6, 12-14] Here, we present *in situ* 2D-IR-SEC using a commercially available optically transparent thin-layer electrochemical (OTTLE) cell, which allows use of a transmission geometry, analogous to traditional linear IR spectroelectrochemical methods.[15] Although this technique does not investigate chemical species at the electrode surface, it does allow for study of post redox species in the bulk solution, in which many of the subsequent steps in the catalytic mechanism occur. In particular, this cell has an aperture in the center platinum working electrode, providing access to a high concentration of reaction intermediates in a region of largely uniform electric field, while avoiding interference from the electrode itself. We also demonstrate how equilibrium 2D-IR dynamics can be obtained in nonequilibrium conditions typical of functioning electrocatalytic devices. This latter point is very important for practical adoption of 2D-IR-SEC because truly steady state conditions will generally not be straightforward to maintain in real-world conditions.

To show 2D-IR-SEC in electrocatalysis, we selected the Lehn catalyst, fac-Re(bpy)(CO)₃Cl, a key CO2 reduction catalyst whose electrochemical intermediates are mostly well established and spectroscopically separated from each other.[16-17] Nevertheless, as discussed below, 2D-IR-SEC enables more direct assignment of spectral features than has been possible with traditional FTIR. The Lehn catalyst has been the subject of numerous studies across multiple disciplines of chemistry since its initial discovery in the 1980s, due to its high selectivity for CO₂ reduction.[18-23] SEC (FTIR and UV-vis) has played a major role in elucidating the electrocatalytic mechanism, revealing both a solvent and ligand dependence for the reduction of the catalyst family fac-Re(4,4'-R₂-bpy)(CO)₃X.[17, 24] Remarkably, this catalyst can act as both a photo- and electrocatalyst for CO2 reduction. Our previous experiments using transient 2D-IR, where a UV or visible pump pulse precedes a 2D-IR probe sequence, determined that the first intermediate of the photocycle, a long-lived ³MLCT state, exhibits different population relaxation and spectral diffusion dynamics relative to the ground state, which we attributed to multiple factors including solvent friction and the modified electronic structure of the catalyst.[25-26] While this change in the electron density due to the ³MLCT was profound, minor changes in electron density around the Re metal center induced through modifications to the bipyridine ligand, do not result in any appreciable changes in the dynamics. We do, however, observe a consistent correlation between

spectral diffusion time scales and the solvent donicity, a metric used to describe the nucleophilicity of the solvent.[27] These results highlight how changes in charge distribution, molecular modifications and solvent environment can affect the observed dynamics. In this work, we build upon our findings of the dynamical behavior of both the ground and triplet excited state of *fac*-Re(bpy)(CO)₃Cl (ReCl), as well as the previously proposed spectroelectrochemically determined mechanisms, to report the first ultrafast 2D-IR measurements on this rhenium catalyst *in situ* during its electrocatalytic reduction, using our novel transmission geometry 2D-IR-SEC experimental design. We also show how this technique is useful for clear identification of chemical intermediates using the spectroscopic signatures of coupled vibrational modes giving rise to specific cross-peaks in the 2D-IR spectrum. In particular, we find direct evidence for Re-Re dimer formation in acetonitrile solvent, a key mechanistic detail that has been a subject of debate.[16, 22-23, 28-29]

2D-IR Spectroscopy Electrochemistry is an inherently non-equilibrium process due to the application of a potential, and the inevitable build-up of intermediates and products, as well as the concomitant loss of reactant species. The quantity of any given species will not influence the ultrafast dynamics unless there are substantial intermolecular interactions, and we presume these to be negligible at typical concentrations (<20 mM). Nevertheless, because the 2D-IR signal is proportional to the number of molecules in the sample, as those change during the chemical reaction, overall signal levels will also change. Therefore, we need a way to monitor the concentrations of chemical species in real time as we collect each 2D spectrum. To adapt our 2D-IR spectrometer (details in the SI) to SEC, we make use of the tracer beam, ordinarily only needed for alignment into the detector, to record a transmission spectrum before scanning each rephasing or nonrephasing 2D-IR spectrum. We block the local oscillator and the three excitation pulses, while unblocking the tracer using opaque cards mounted on servo motors. The transmission spectrum is computed as the average of 50 laser shots. Dividing each transmission spectrum by the blank tracer spectrum and computing the negative logarithm gives the absorption spectrum (Fig. S1). These spectral features agree with the FTIR absorbance measured prior to and immediately following the 2D-IR-SEC experiments. The individual scan absorbance values are used to scale the rephasing and nonrephasing peak amplitudes for each t2 value, allowing for effectively equilibrium dynamical information in an overall nonequilibrium chemical reaction. We compared this scaling technique to the situation carefully prepared at a truly steady-state (i.e. constant) concentration, and obtained identical dynamical behavior (vide infra). We are confident that this scaling approach can be applied to systems where concentrations change on a timescale comparable to or longer than each of the rephasing/nonrephasing scans (~1 minute in our spectrometer). This approach is general, and represents an advance in the field of 2D-IR, where we anticipate more important applications will involve globally nonequilibrium conditions, similar to 2D-IR spectroscopic probes of nonequilibrium phenomena such as protein aggregation.[30]

Sample Preparation Re(bpy)(CO)₃Cl (ReCl) was synthesized according to published methods. Anhydrous THF, anhydrous acetonitrile (ACN), tetrabutylammonium hexafluorophosphate (TBAPF₆) and tetrabutylammonium chloride (TBACl) were obtained from Sigma Aldrich and used as received. An IR OTTLE cell (Frantisek Hartl, University of Reading), equipped with Pt-minigrid working and auxiliary electrodes, a Ag-wire pseudoreference electrode, which are melt-sealed into a polyethylene spacer (200 μ m), and 2-mm thick CaF₂ windows, was employed for the SEC measurements (**Fig. 1**).[15] Cyclic voltammetry and controlled potential amperometry within the

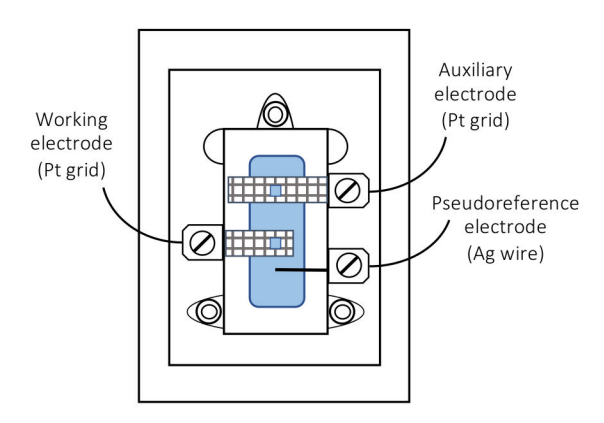


Figure 1 Top-down view of the OTTLE cell used for 2D-IR spectroelectrochemistry of CO_2 reduction electrocatalyst, $Re(bpy)(CO)_3CI$. The holes in the Pt mesh grids enable scatter-free transmission of the beams used in 2D-IR.

OTTLE cell were carried out using a PalmSens EmStat3 potentiostat. FTIR-SEC spectra were measured using a JASCO 4100 spectrometer. For all SEC experiments, the concentration of ReCl was 10 mM, and the concentration of either electrolyte used was 0.1 M in the solvent. All SEC experiments were conducted in an atmosphere free of air by sparging with Ar for 20 minutes prior to SEC measurements. All potentials reported are against the internal standard redox couple Fc/Fc⁺.

Linear FTIR Measurements Previous SEC experiments generated and reported the identity of the intermediate species and their corresponding vibrational frequencies, [17, 24] leading to the proposed initial mechanism shown in Figure 2A. Upon addition of the first electron to the catalyst, an anionic species forms (2) which can then lose Cl^- , forming either a five-coordinated radical species (3), or a solvato radical species (4). (3) goes on to form a Re-Re dimer (5) or undergoes a second reduction to become species (7), which is considered the catalytically active species for the 2-electron CO_2 reduction catalysis reaction.[31] The specific pathway depends on the solvent, which can stabilize or destabilize some intermediates. To showcase our new 2D-IR-SEC technique, this Letter focuses on the intermediates leading up to the formation of the catalytically active species. Future work will focus on the full electrocatalytic reduction of CO_2 .

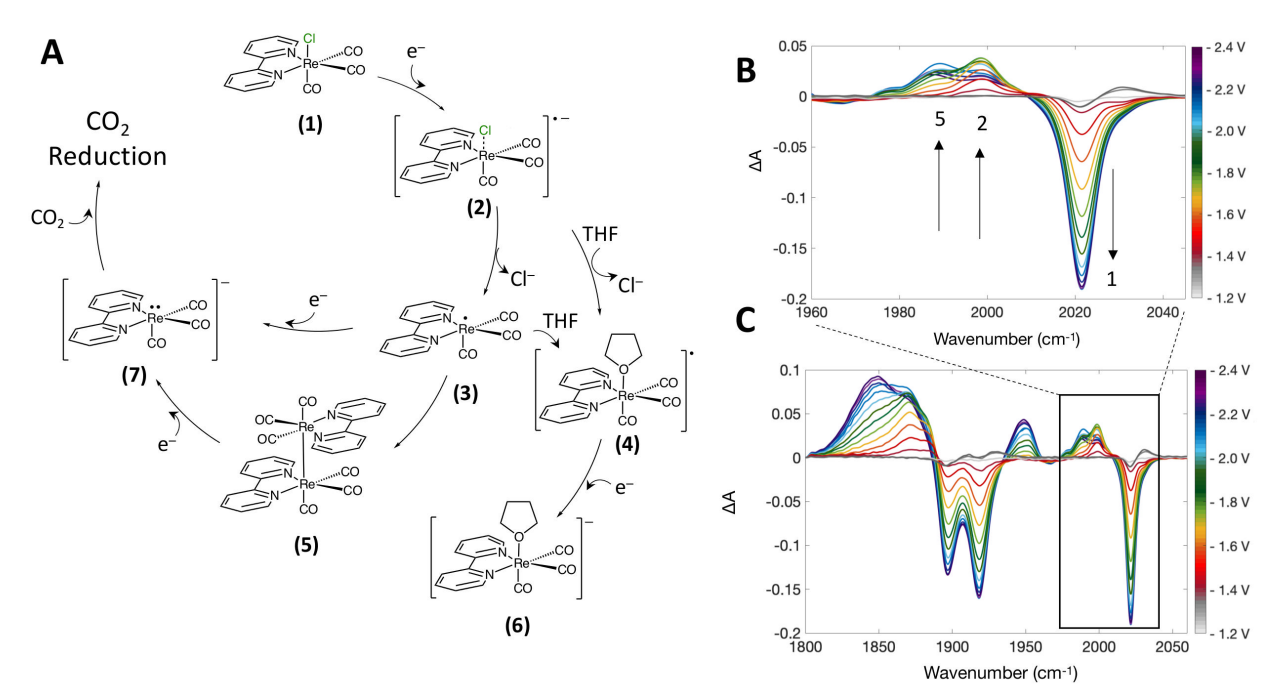


Figure 2 (A) Proposed initial mechanism of the Re(bpy)(CO) $_3$ Cl (ReCl) electrocatalytic reduction cycle in THF adapted from references 16 and 17. (B) FTIR difference spectra (0 V spectrum subtracted from spectra with applied voltage) of the A'(1) modes of the starting complex ReCl (1), the singly reduced species (2), and the Re-Re dimer (5) in THF with 0.1 M TBAPF $_6$ over a voltage range of -1.2 to -2.4 V (vs. Fc/Fc $^+$). (C) FTIR difference spectra of all three of the carbonyl stretching modes in THF with 0.1 M TBAPF $_6$ over a voltage range of -1.2 to -2.4 V (vs. Fc/Fc $^+$).

Linear FTIR-SEC measurements using the OTTLE cell (**Fig. 2B,C**) displayed as difference spectra are consistent with previous reports. The voltage was stepped down in increments of 0.1 V for 5 minutes each covering a range from -1.2 V to -2.4 V (vs. Fc/Fc⁺). The characteristic carbonyl peaks from the starting complex, ReCl (**1**) in THF, appear at 2019, 1917, and 1894 cm⁻¹.[17] As the applied voltage becomes more negative, peaks assigned to the singly reduced species (**2**) begin to grow in at 1996, 1883, and 1868 cm⁻¹. As the voltage is further decreased, signatures from the dimer species (**5**) distinctly appear at 1986 and 1950 cm⁻¹. There is evidence of the lower frequency modes of the dimer at 1887 and 1857 cm⁻¹, however, in the linear spectra, it becomes difficult to separate the peaks unambiguously in that region given the overlap with the lower frequency modes of the singly and doubly reduced species. The high-frequency mode of the doubly reduced species (**6**) appears at 1947 cm⁻¹ with a second broad absorption at 1843 cm⁻¹, and is clearly seen in the dark purple spectrum of **Fig. 2C**.

2D-IR-SEC Measurements 2D-IR experiments were conducted under the same conditions as the linear IR-SEC experiments: $10 \text{ mM} \text{ Re(bpy)(CO)}_3\text{Cl in a } 0.1 \text{ M TBAPF}_6$ electrolyte solution in THF. We report only the high frequency, A'(1) band at ~2019 cm⁻¹, as it is well separated from the lower bands (**Fig. 2B**), and exhibits diagnostic shifts for the intermediate species allowing a straightforward interpretation of the dynamics. The applied potential of -2.1 V was selected by performing cyclic voltammetry and choosing a potential more negative than the first reduction potential ($E_{1/2}$ =1.83 V vs Fc/Fc⁺) (Figure S2).

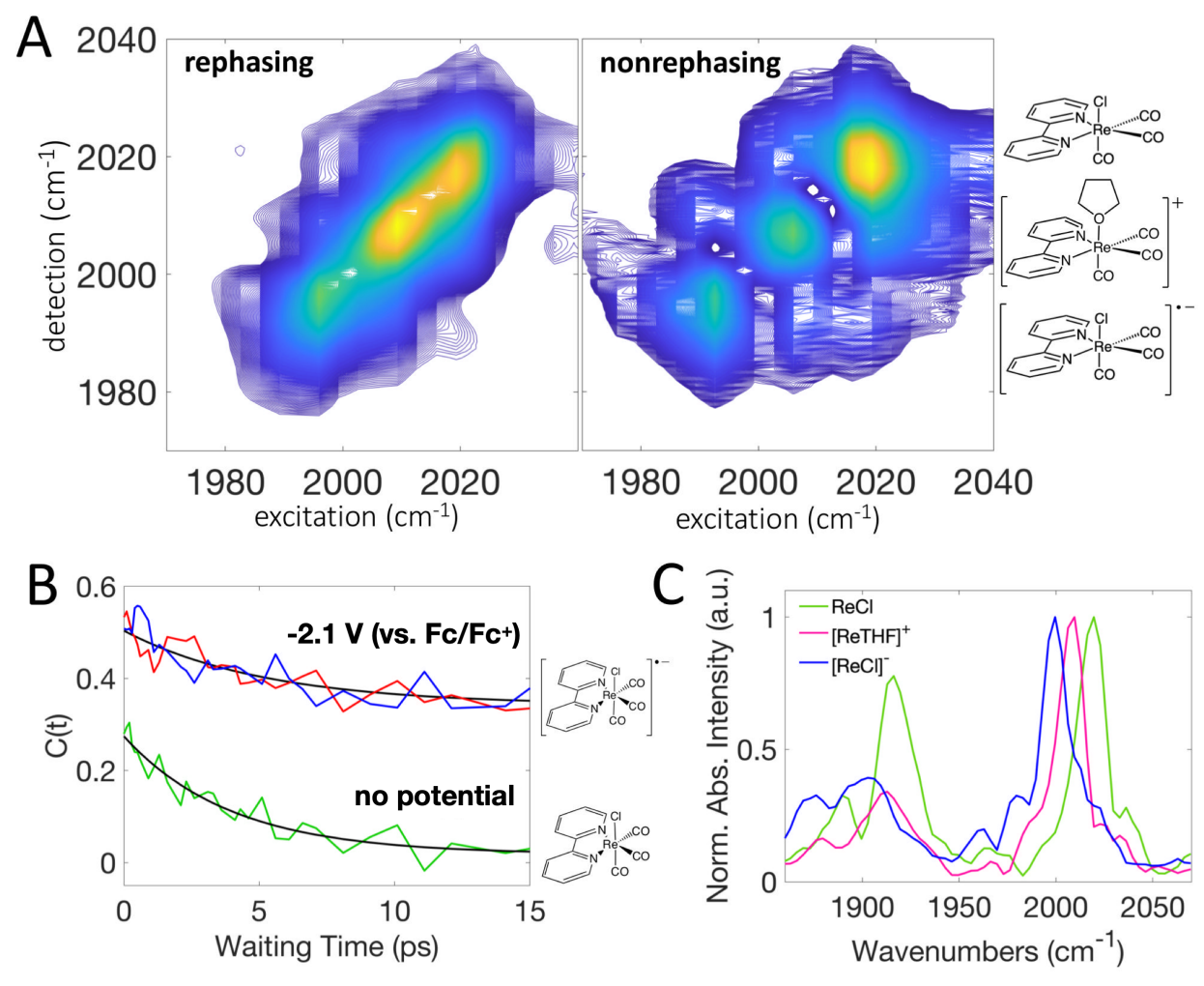


Figure 3 (A) Absolute value rephasing (left) and nonrephasing (right) spectra (t_2 = 200 fs) of the intermediate species after -2.1 V is applied to ReCl with 0.1M TBAPF₆ in THF. The reduced species, [Re(bpy)(CO)₃Cl]^{•-}, appears at 1996 cm⁻¹, the band at ~2010 cm⁻¹ is from a solvato cationic species, [Re(bpy)(CO)₃THF]⁺, resulting from the reduced species interacting with O₂, and the band at 2019 cm⁻¹ is from the starting material, Re(bpy)(CO)₃Cl. (B) A comparison of the frequency fluctuation correlation function, C(t), for the reduced species from a steady-state experiment (blue), an absorbance-scaled nonequilibrium experiment (red), and the starting material (green) showing the reduced species having a slower correlation decay time than the neutral starting material. (C) Slices from the absolute value non-rephasing spectrum (t_2 = 100 fs), at detection frequencies corresponding to the three species indicated in (A), low-frequency modes resolved as cross peaks to the high-frequency modes become visible due to vibrational coupling.

The primary dynamical measurement is the determination of the frequency-fluctuation correlation function (FFCF, or C(t)), which decays due to the loss of frequency memory induced by equilibrium solvation dynamics known as "spectral diffusion." We use the inhomogeneity index method (described in the SI) to obtain the FFCF from a waiting time (t_2) series of rephasing and nonrephasing absolute value spectra. The spectral diffusion decay time of the A'(1) band of the starting material, ReCl in the electrolyte solution, was determined to be slower (4.0 \pm 0.9 ps) than that of the same complex in neat THF (3.1 ± 0.4 ps), though we observe no solvatochromism or broadening of the CO stretching modes due to the addition of the electrolyte.[25-27] A concentration dependence study shows that the slowdown occurs at less than a 1:1 ratio of complex to electrolyte, indicating a strong preferential solvation of the electrolyte around the complex relative to neat THF (Figure S3). With an applied voltage of -2.1 V, the intermediate species are not observable until roughly 10 minutes elapsed time, though these species are

observed at less negative potentials in the linear FTIR experiments (**Fig. 2C**). To test the reliability of the tracer absorption correction procedure, we carried out 2D-IR-SEC under two conditions: one in which the reduced species is in a true steady-state, and the other in which the reduced species population changes over time because steady state had not been established.

Figure 3A shows an absolute rephasing and nonrephasing spectrum after a potential of -2.1 V was applied for tens of minutes, with a waiting time delay (t_2) of 200 fs. Additionally, we recorded a 2D-IR-SEC experiment under nonequilibrium conditions with the potential held at -2.1 V, waiting only a few minutes before starting the 2D-IR sequence. The resulting amplitudes of the diagonal peaks in the rephasing and nonrephasing spectra at each waiting time delay are individually scaled to the corresponding calculated absorbance. We use these scaled amplitudes to compute the inhomogeneity index (Fig. 3B). The FFCF data for both steady-state and nonequilibrium conditions overlap, confirming that the absorption correction method works. The equilibrium spectral diffusion decay of the reduced species, fit with a single exponential and constant offset, is slower (5.5 \pm 2.1 ps) than that of the starting material in the electrolyte solution. The reduced species has a larger initial FFCF ($C(0) = \langle (\delta \omega)^2 \rangle$) than the starting complex; given essentially identical FTIR spectra widths, the larger initial correlation indicates a larger inhomogeneous width for the reduced species. In the reduced species, there is a reproducible offset of ~0.3 that is not present in the starting material ReCl A'(1) peak from the same experiment, indicating static heterogeneity or dynamics slower than our measurement range. The solvation environment is already somewhat complex for the starting ReCl alone due to the presence of 0.1 M electrolyte, and the situation becomes even more electrostatically rich upon reduction to a radical anion. We attribute the long time dynamics to the strong interactions between the reduced species and the electrolyte that preferentially solvates it, as the ionic interactions are stronger than the ion-dipole that occur for the neutral species and may have long-lasting local minima solvation configurations. We anticipate that characterizing solvation dynamics changes during electrocatalysis will be a major area of future research with this new spectroscopy approach, as these transient intermediate species are often difficult or impossible to access under operational conditions.

When the frequencies of the vibrational bands are not known explicitly due to congestion of bands in the spectrum, such as the lower carbonyl stretching modes in this system, a horizontal slice at a specific detection frequency of the high frequency region can be taken to obtain peaks at the corresponding coupled lower-frequency modes. While the peak location for the lower frequency modes is accurate for the slices, the amplitudes are shaped by the excitation pulse spectral bandwidth, which deemphasizes the lower frequency modes. Horizontal slices (Fig. 4B) through each of the high frequency modes of the individual species of (1), (2) and a third cationic species, [Re(bpy)(CO)₃THF]⁺, that results from the reduced species reacting with oxygen that can seep into the system over time, provide unobstructed access to the lower mode frequencies for each species (details in the SI). While having a species generated from oxygen contamination is not desired for the catalysis reaction, this spectrum was selected to highlight the resolving capabilities of the nonrephasing spectrum because these three species are roughly 10 cm⁻¹ apart (Fig. 3A), and would not be better resolved in an absorptive spectrum.

In addition to obtaining equilibrium dynamics from a non-equilibrium system, our 2D-IR-SEC implementation offers new mechanistic insight by clearly identifying redox intermediates. In traditional IR-SEC experiments, complications of assignments arise when spectral bands overlap. Early waiting time (t_2) 2D-IR spectra exhibit cross-peaks due to vibrational coupling among modes of individual chemical species. These cross-peaks assist direct assignment of the vibrational bands

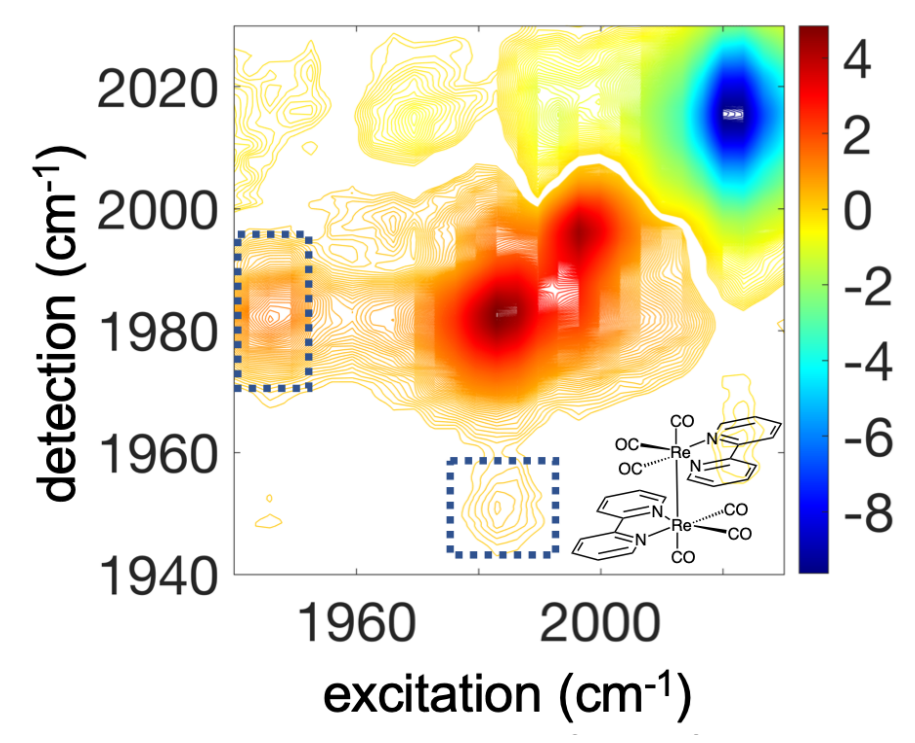


Figure 2 $Re(bpy)(CO)_3CI$ in acetonitrile with TBACI electrolyte at -1.6 V (vs. Fc/Fc⁺). Difference 2D-IR-SEC rephasing spectrum (voltage on – voltage off) at a waiting time of 100 fs. The dashed boxes highlight the cross-peaks, confirming both bands at 1948 and 1986 cm⁻¹ belong to the same species, the Re-Re dimer (5). This spectrum provides direct experimental evidence for the Re-Re dimer in acetonitrile.

that are otherwise obscured by spectral overlap. Turner et al. performed IR-SEC experiments on Re(bpy)(CO)₃Cl in ACN with the electrolyte TBACl and concluded that in this particular system, no dimer formed and assigned the peaks at 1986 and 1948 cm⁻¹ to the anions Re(bpy)(CO)₃(CH₃CN)]⁻ and Re(bpy)(CO)₃]-, respectively.[17] Siewart et al. repeated the experiment in both ACN and DMF and assigned these same peaks to the Re-Re dimer based on previously reported calculations.[28, 32-33] Although calculations are often indispensable, experimental observation of the cross-peaks is an unambiguous method of species identification, provided the spectral features can be assigned. Figure 4 shows a 2D-IR-SEC difference spectrum of 10 mM Re(bpy)(CO)₃Cl in ACN (at -1.6 V vs. Fc/Fc⁺) with 0.1 M TBACl (Ar purged) at a waiting time of 100 fs. The pronounced cross-peaks between the modes at 1948 and 1986 cm⁻¹ are assigned to the dimer species (5). The effectiveness of a catalyst is determined by the turnover number (i.e. yield per catalyst molecule) and turnover frequency (i.e. the conversion rate). The dimer represents a bottleneck in the electrocatalytic mechanism, since its formation requires a further two-electron reduction to generate the five-coordinate diradical anion.[29] Our 2D-IR-SEC results experimentally resolve the presence of this dimer species in acetonitrile, new information that can guide the refinement of next-generation rhenium-diimine electrocatalysts.

Conclusion This work highlights a powerful new capability of applying 2D-IR to electrochemistry, both in steady state and *in situ* conditions using an OTTLE cell and a transmission geometry. We have demonstrated that it is possible to obtain equilibrium dynamics in non-equilibrium conditions and to generate electrochemical intermediates that have previously been difficult to access with ultrafast measurements. The electrolyte, TBAPF₆, exhibits strong preferential solvation of the Re complex, creating a microenvironment that slows the spectral diffusion relative to the neat solvent case. In the first *in situ* 2D-IR-SEC measurements performed on the ReCl/electrolyte mixture, we report an even slower spectral diffusion for the singly reduced species than for the neutral starting material, likely reflecting the complex motional dynamics of electrolytes in the vicinity of a charged, dipolar organometallic complex. In the spectra themselves, we observe cross-peaks between carbonyl stretching modes of the intermediate dimer species, [Re(bpy)(CO)₃]₂, resolving a mechanistic debate, while demonstrating the use of 2D-IR-SEC as a powerful tool for species identification during an electrochemical reaction. Future work will focus on the full CO₂ reduction reaction, as well as the influence of solvents, electrolytes and chemical substituents on the catalyst.

ASSOCIATED CONTENT

Supporting Information

The Supporting Information is available free of charge at XXX.

Experimental methods; Absorption determination; Cyclic voltammetry; FFCF of varying concentrations of TBAPF₆; Steady-state and nonequilibrium [ReCl]⁻; FTIR of ReCl in 0.1M TBAPF₆; Inhomogeneity index and FFCF; Determination of lower frequency mode locations; and additional references.

Notes

The authors declare no competing financial interest.

Acknowledgements

This work was supported by the National Science Foundation (CHE-1836529 and CHE-1955026).

References

- 1. Jeanmaire, D. L.; Vanduyne, R. P., Surface Raman Spectroelectrochemistry .1. Heterocyclic, Aromatic, and Aliphatic-Amines Adsorbed on Anodized Silver Electrode. *J. Electroanal. Chem.* **1977**, *84*, 1-20.
- 2. Klod, S.; Ziegs, F.; Dunsch, L., In Situ NMR Spectroelectrochemistry of Higher Sensitivity by Large Scale Electrodes. *Anal. Chem.* **2009**, *81*, 10262-10267.
- 3. Boisseau, R.; Bussy, U.; Giraudeau, P.; Boujtita, M., In Situ Ultrafast 2D NMR Spectroelectrochemistry for Real-Time Monitoring of Redox Reactions. *Anal. Chem.* **2015**, *87*, 372-375.
- 4. Ibanez, D.; Garoz-Ruiz, J.; Heras, A.; Colina, A., Simultaneous UV-Visible Absorption and Raman Spectroelectrochemistry. *Anal. Chem.* **2016**, *88*, 8210-8217.

- 5. Domingos, S. R.; Luyten, H.; van Anrooij, F.; Sanders, H. J.; Bakker, B. H.; Buma, W. J.; Hartl, F.; Woutersen, S., An optically transparent thin-layer electrochemical cell for the study of vibrational circular dichroism of chiral redox-active molecules. *Rev. Sci. Instrum.* **2013**, *84*, 033103.
- 6. El Khoury, Y.; van Wilderen, L.; Bredenbeck, J., Ultrafast 2D-IR Spectroelectrochemistry of Flavin Mononucleotide. *J. Chem. Phys.* **2015**, *142*, 212416.
- 7. Khalil, M.; Demirdoven, N.; Tokmakoff, A., Coherent 2D IR spectroscopy: Molecular structure and dynamics in solution. *J. Phys. Chem. A* **2003**, *107*, 5258-5279.
- 8. Baiz, C. R.; Mcrobbie, P. L.; Anna, J. M.; Geva, E.; Kubarych, K. J., Two-Dimensional Infrared Spectroscopy of Metal Carbonyls. *Acc. Chem. Res.* **2009**, *42*, 1395-1404.
- 9. Kiefer, L. M.; Kubarych, K. J., Solvent Exchange in Preformed Photocatalyst-Donor Precursor Complexes Determines Efficiency. *Chem. Sci.* **2018**, *9*, 1527-1533.
- 10. Maekawa, H.; Sul, S.; Ge, N.-H., Vibrational Correlation Between Conjugated Carbonyl and Diazo Modes Studied by Single- and Dual-Frequency Two-Dimensional Infrared Spectroscopy. *Chem. Phys.* **2013**, *422*, 22-30.
- 11. Eckert, P. A.; Kubarych, K. J., Oxidation-State-Dependent Vibrational Dynamics Probed with 2D-IR. *J. Phys. Chem. A* **2017**, *121*, 2896-2902.
- 12. Lotti, D.; Hamm, P.; Kraack, J. P., Surface-Sensitive Spectro-electrochemistry Using Ultrafast 2D ATR IR Spectroscopy. *J. Phys. Chem. C* **2016**, *120*, 2883-2892.
- 13. Kraack, J. P.; Hamm, P., Surface-Sensitive and Surface-Specific Ultrafast Two-Dimensional Vibrational Spectroscopy. *Chem. Rev.* **2017**, *117*, 10623-10664.
- 14. El Khoury, Y.; Van Wilderen, L.; Vogt, T.; Winter, E.; Bredenbeck, J., A Spectroelectrochemical Cell for Ultrafast Two-Dimensional Infrared Spectroscopy. *Rev. Sci. Instrum.* **2015**, *86*, 083102.
- 15. Hartl, F.; Luyten, H.; Nieuwenhuis, H. A.; Schoemaker, G. C., Versatile Cryostated Optically Transparent Thin-Layer Electrochemical (OTTLE) Cell for Variable-Temperature UV-Vis IR Spectroelectrochemical Studies. *Appl. Spectrosc.* **1994**, *48*, 1522-1528.
- 16. Stor, G. J.; Hartl, F.; Vanoutersterp, J. W. M.; Stufkens, D. J., Spectroelectrochemical (IR, UV/VIS) Determination of the Reduction Pathways for a Series of Re(CO)₃(Alpha-Diimine)L' (0/+) (L'=Halide, OTF⁻, THF, MeCN, N-PRCN, PPH₃, P(OMe)₃) Complexes. *Organometallics* **1995**, *14*, 1115-1131.
- 17. Johnson, F. P. A.; George, M. W.; Hartl, F.; Turner, J. J., Electrocatalytic Reduction of CO_2 Using the Complexes Re(bpy)(CO_3L^n (n=+1, L=P(OEt)₃, CH₃CN; n=0, L=Cl-, Otf(-); bpy=2,2'-bipyridine; Otf₋=CF₃SO₃) as catalyst precursors: Infrared Spectroelectrochemical investigation. *Organometallics* **1996**, *15*, 3374-3387.
- 18. Hawecker, J.; Lehn, J. M.; Ziessel, R., Efficient Photochemical Reduction Of CO₂ to CO By Visible-Light Irradiation of Systems Containing Re(bipy)(CO)₃X Or Ru(bipy)₃²⁺-Co²⁺ Combinations as Homogeneous Catalysts. *J. Chem. Soc., Chem. Commun.* **1983**, 536-538.
- 19. Hawecker, J.; Lehn, J. M.; Ziessel, R., Electrocatalytic Reduction of Carbon-Dioxide Mediated by Re(bipy)(CO)₃Cl(bipy=2,2'-bipyridine). *J. Chem. Soc., Chem. Commun.* **1984**, 328-330.
- 20. Sullivan, B. P.; Bolinger, C. M.; Conrad, D.; Vining, W. J.; Meyer, T. J., One-Electron and 2-Electron Pathways in the Electrocatalytic Reduction Of CO_2 by fac-Re(2,2'-bipyridine)(CO)₃Cl. *J. Chem. Soc., Chem. Commun.* **1985**, 1414-1415.
- 21. Breikss, A. I.; Abruna, H. D., Electrochemical and Mechanistic Studies of $Re(CO)_3(dmbpy)Cl$ and their Relation to the Catalytic Reduction of CO_2 . *J. Electroanal. Chem.* **1986**, *201*, 347-358.

- 22. O'Toole, T. R.; Sullivan, B. P.; Bruce, M. R. M.; Margerum, L. D.; Murray, R. W.; Meyer, T. J., Electrocatalytic Reduction of CO₂ by a Complex of Rhenium in Thin Polymeric Films. *J. Electroanal. Chem.* **1989**, *259*, 217-239.
- 23. Christensen, P.; Hamnett, A.; Muir, A. V. G.; Timney, J. A., An *in situ* Infrared Study of CO₂ Reduction Catalyzed by Rhenium Tricarbonyl Bipyridyl Derivatives. *J. Chem. Soc., Dalton Trans.* **1992**, 1455-1463.
- 24. Smieja, J. M.; Kubiak, C. P., Re(bipy-tBu)(CO)₃Cl-improved Catalytic Activity for Reduction of Carbon Dioxide: IR-Spectroelectrochemical and Mechanistic Studies. *Inorg. Chem.* **2010**, *49*, 9283-9289.
- 25. Kiefer, L. M.; King, J. T.; Kubarych, K. J., Equilibrium Excited State Dynamics of a Photoactivated Catalyst Measured with Ultrafast Transient 2DIR. *J. Phys. Chem. A* **2014**, *118*, 9853-9860.
- 26. Kiefer, L. M.; King, J. T.; Kubarych, K. J., Dynamics of Rhenium Photocatalysts Revealed through Ultrafast Multidimensional Spectroscopy. *Acc. Chem. Res.* **2015**, *48*, 1123-1130.
- 27. Kiefer, L. M.; Kubarych, K. J., Solvent-Dependent Dynamics of a Series of Rhenium Photoactivated Catalysts Measured with Ultrafast 2DIR. *J. Phys. Chem. A* **2015**, *119*, 959-965.
- 28. Hayashi, Y.; Kita, S.; Brunschwig, B. S.; Fujita, E., Involvement of a binuclear species with the Re-C(O)O-Re moiety in CO_2 reduction catalyzed by tricarbonyl rhenium(I) complexes with diimine ligands: Strikingly slow formation of the Re-Re and Re-C(O)O-Re species from Re(dmb)(CO)₃S (dmb=4,4'-dimethyl-2,2'-bipyridine, S = solvent). *J. Am. Chem. Soc.* **2003**, *125*, 11976-11987.
- 29. Benson, E. E.; Kubiak, C. P., Structural investigations into the deactivation pathway of the CO₂ reduction electrocatalyst Re(bpy)(CO)₃Cl. *Chem. Commun.* **2012**, *48*, 7374-7376.
- 30. Shim, S. H.; Gupta, R.; Ling, Y. L.; Strasfeld, D. B.; Raleigh, D. P.; Zanni, M. T., Two-dimensional IR spectroscopy and isotope labeling defines the pathway of amyloid formation with residue-specific resolution. *Proc. Natl. Acad. Sci. U. S. A.* **2009**, *106*, 6614-6619.
- 31. Sampson, M. D.; Froehlich, J. D.; Smieja, J. M.; Benson, E. E.; Sharp, I. D.; Kubiak, C. P., Direct Observation of the Reduction of Carbon Dioxide by Rhenium Bipyridine Catalysts. *Energy Environ. Sci.* **2013**, *6*, 3748-3755.
- 32. Du, J. P.; Siewert, I., An Electrochemical and Spectroscopic Study on $Re(CO)_3(L)Cl$ in Dimethylformamide (L=2,2'-Bipyridine). *Z. Anorg. Allg. Chem.* **2020**, *646*, 705-711.
- 33. Fujita, E.; Muckerman, J. T., Why is Re-Re bond formation/cleavage in $[Re(bpy)(CO)_3]_2$ different from that in $[Re(CO)_5]_2$? Experimental and theoretical studies on the dimers and fragments. *Inorg. Chem.* **2004**, *43*, 7636-7647.